Published in final edited form as:
J Mass Spectrom. 2009 April ; 44(4): 477–484. doi:10.1002/jms.1523.

Peptide Fragmentation Induced by Radicals at Atmospheric Pressure

Andrey N. Vilkov, **Victor V. Laiko**, and **Vladimir M. Doroshenko**
MassTech, Inc., Columbia, MD, USA

Abstract

A novel ion dissociation technique, which is capable of providing an efficient fragmentation of peptides at essentially atmospheric pressure conditions, is developed. The fragmentation patterns observed often contain c-type fragments that are specific to ECD/ETD, along with the y-/b- fragments that are specific to CAD. In the presented experimental setup, ion fragmentation takes place within a flow reactor located in the atmospheric pressure region between the ion source and the mass spectrometer. According to a proposed mechanism, the fragmentation results from the interaction of ESI-generated analyte ions with the gas-phase radical species produced by a corona discharge source.

Keywords

ion fragmentation; atmospheric pressure; hydroxyl radicals; electron capture dissociation; electron transfer dissociation

Introduction

Tandem mass spectrometry (MS/MS) currently claims a key role in the identification and characterization of proteins [1–7]. Successful mass spectrometric analysis of peptides and proteins relies on the ability to systematically sever peptide backbone bonds. In conventional collision-activated dissociation (CAD) MS/MS, ion fragmentation is activated by collisions with a buffer gas [8]. However, acquiring structural information through this method becomes significantly more challenging when the peptide is substantially long (more than approximately 20 residues [9]) or contains either labile post-translational modifications or multiple basic residues.

Alternative fragmentation methods, electron capture dissociation (ECD) [10] and electron transfer dissociation (ETD) [11–13], have been recently introduced into the field of proteomics. Unlike the collision-activated process, ECD and ETD do not cleave chemical modifications from the peptide, but rather induce random breakage of the peptide backbones. ECD and ETD can be used as orthogonal (to standard CAD) fragmentation methods to increase the informational content of tandem MS experiments. In spite of the remarkable prospects for proteomics, these techniques have been primarily implemented only in mass spectrometers that have ion traps such as Fourier Transform Ion Cyclotron Resonance (ECD case) and radiofrequency linear ion trap (ETD case) mass spectrometers.

Historically, experiments employing ECD/ETD-type fragmentation have been conducted inside a vacuum system with an operating pressure of no more than 1 mTorr. However, ion/

Correspondence should be addressed to: Dr. Andrey N. Vilkov, MassTech Inc., 6992 Columbia Gateway Drive, Columbia, MD 21046, USA, Email: E-mail: andrey_vilkov@apmaldi.com.

ion and ion/molecule reactions can be very efficient even at atmospheric pressure. For instance, the use of proton-transfer reactions at the essentially atmospheric pressure is, nowadays, the most straightforward route to charge reduction of multiply charged peptides and proteins generated by electrospray. The effectiveness of this approach was first demonstrated by Orgozalek et al in 1992 by coupling the output of an electrospray with an externally housed corona discharge source [14]. Later, methods merging electrosprayed cations with corona discharged anions have been seriously modified and successfully demonstrated [15–18]. Recently, our group has reported the fragmentation of peptides at essentially atmospheric pressure conditions achieved by merging electrosprayed peptide ions with corona generated radicals [19].

In this paper, we further explore the developed ion dissociation technique which is capable of providing efficient fragmentation of peptides and proteins with typical patterns containing fragments specific to both CID and ECD/ETD. In the presented experimental setup, ion dissociation occurs within the flow reactor, located in the atmospheric pressure region between the ion source and the mass spectrometer. The suggested fragmentation mechanism involves the interaction of ESI-generated peptide ions with hydroxyl radicals originating from the corona discharge source.

Experimental

All experiments were performed using an LCQ “Classic” instrument (Thermo Scientific, San Jose, CA). The analyte ions were produced by ESI and the radical species were produced by corona discharge. The analyte ions and radical species were mixed together within the stainless steel flow reactor, shown in Figure 1. The internal diameter of the flow reactor was smaller at the entrance (0.5 mm i.d.) and larger at the mixing region (2.5 mm i.d.). Similar design was used for proton-transfer reactions near atmospheric pressure by Frey et al [20]. The chosen dimensions should cause minimal pressure drop through the reactor, since the majority of the pressure decrease occurs at the long and narrow capillary of MS instrument. The geometry of the flow reactor defines the gas flow velocity through out the mixing region, thus dictating the ion-molecule interaction time.

Two standard cartridge heaters (80W, ¼”o.d., McMaster-Carr, Dayton, NJ) were used to vary the temperature of the flow reactor in the range 20–500°C. The temperature of the flow reactor was measured by inserted Nextel coated J-type thermocouple and moderated by a temperature controller (Model CN9110A, Omega Engineering, Stamford, CT). The temperature of the gas flowing through the corona discharge was adjusted separately using a coiled tube wrapped with band heaters (McMaster-Carr, Dayton, NJ, not shown in Figure 1).

The front-end of the flow reactor had a counter-current flow of “curtain” gas (nitrogen) to aid the desolvation of droplets generated by ESI and to sweep away unwanted neutral species from the entrance aperture. The flow reactor was tightly seated onto the heated capillary of the MS instrument with a ceramic holder that provides a separation distance of 0.5 mm between the body of reactor and the heated capillary. To improve ion transmission through the reactor into MS instrument, a variable DC voltage was applied to the body of flow reactor (typically 50–150 V).

Corona discharge was utilized for ion/radical generation. A custom-built metal tee was installed into the stainless steel body of the flow reactor. The top end of the tee connector held a ceramic tube with platinum wire inside. The side port (1/8” Swagelock) of the tee connector was used to provide a constant flow of reagent gas through the source. The platinum wire (0.004” o.d., Scientific Instrument Services, Ringoes, NJ) was held at a few kilovolts (typically 2 kV) potential relative to the flow reactor. The corona discharge was created between the sharpened tip of the platinum wire and stainless steel disk having a small orifice (typically 1 mm)

separating the corona discharge region from the flow reactor that lay in the counter bore made in the body of the flow reactor. A power supply (model PS350, Stanford Research, Sunnyvale, CA) was used to apply a high voltage and to limit a current within the corona discharge source. A gas flow meter (T-type meter, Aalborg, Orangeburg, NY) was used to control the flow rate (0–500 cm^3/min) of the reaction gas through the corona discharge region.

Electrospray ionization was employed to produce positively and negatively charged peptide and proteins ions. The solutions were infused into the ESI source (50 μm i.d. fused silica capillary with +/− 2.5 kV voltage applied to the solution via a coupling metal HPLC union) at a rate of 1 μl/min using a syringe pump (Model 11 plus, Harvard Apparatus, MA).

The peptides and proteins purchased from Sigma (St. Louis, MO) and American Peptides, Inc. (Sunnyvale, CA) were dissolved in a solution containing 49% water, 49% methanol and 2% acetic acid. The peptide concentrations used in the ESI experiments were in the range of 5 – 25 μM. All UHP grade reaction gasses (Ar, He, SO_2, O_2 and N_2) and dry compressed air were purchased from Airgas East (Hyattsville, MD).

Results and discussion

Ion/molecule reaction time

The internal diameter of LCQ “Classic” heated capillary is 0.5 mm therefore this dimension dictates the gas flow rate throughout the flow reactor. The gas flow rate (G) was precisely measured at room temperature to be 1020 cc/min. The average linear gas speed (*v*) through flow reactor can be calculated using a simple relationship:

$$v=\frac{4G}{\pi d^2} \tag{1}$$

that gives an average gas flow speed of 3.5 m/s through the central channel (2.5 mm i.d.). Thus, a residence time (and therefore ion/molecule reaction time) can be estimated to be approximately 10 ms.

Ion transmission efficiency

To calculate an ion transmission through the flow reactor of the proposed design, one can apply the approximated formula derived by Konenkov *et al* for the fraction of ions lost by diffusion to the walls [21]:

$$\frac{I}{I_0}=exp\left[-5.784\cdot\left(\frac{2L}{d}\right)^2\frac{kT}{qU_{eff}}\right] \tag{2}$$

where *I* is the transmitted current, I_0 is the entrance ion current, *L* is the length of the chamber, *d* is the diameter of the chamber, *k* is Boltzmann’s constant, *T* is the temperature, *q* is the ion charge and U_{eff} is the effective potential difference down the length of the chamber. Since ion mobility through the chamber is controlled by the gas flow, the effective potential U_{eff} is given by equation 3 [22]:

$$U_{eff}=\frac{vL}{K} \tag{3}$$

where *v* is the average gas flow speed and *K* is the ion mobility. Using the values calculated above and K=1cm^2/Vs (typical ion mobility), equation 2 gives an ion transmission efficiency at room temperature through the proposed flow reactor of approximately 95.8%.

According to equation 2, the elevated temperature of the flow reactor would result in an ion transmission drop with a temperature increase. For example, an increase in temperature to 200° C will decrease ion transmission down to 93% which still can be considered as relatively high.

Charge reduction of ions formed in ESI source at elevated temperatures

The mean charge state of electrosprayed peptide and protein ions depends on the experimental conditions, such as solvent used. We assume that the temperature of the background gas also affects the charge state distribution through the following mechanism. The maximum surface charge density of ESI droplets sustained by a given liquid depends on its surface tension [23]. In the case of charged spherical droplets, this is given by [24]:

$$N^2e^2=8\pi^2\varepsilon_0 D^3\sigma \quad (4)$$

where *N* is the number of charges, *e* is the elementary charge, ε_0 is the permittivity of the surrounding medium, *D* is the diameter of the droplet at which droplet instability occurs (the Rayleigh limit) and σ is the surface tension. For a given solvent, all of these parameters are constants except surface tension that is dependant on temperature. The general trend is that surface tension decreases with the increase of temperature, reaching a value of 0 at the critical temperature (T_c). There are only empirical equations to relate surface tension and temperature, such as Guggenheim-Katayama equation [25]:

$$\sigma=\sigma_0\left(1-\frac{T}{T_c}\right)^n \quad (5)$$

Thus, the maximum charge state of ESI ions decreases with an increase in the temperature of the surrounding medium.

To confirm this hypothesis, we have experimentally studied the temperature effect on the charge distribution for a variety of peptides and proteins and found a pronounced charge reduction with temperature. The typical charge state distribution of ESI-generated Substance P ions as a function of flow reactor temperature is shown in Figure 2. In the temperature range of 380–440°C, used in all fragmentation experiments, we observed only single-charged peptide ions. No ion signal was observed for temperatures more than 440°C.

Experimental results

For any new dissociation technique, fragmentation of Substance P ions is, nowadays, a general benchmark test. Figure 3a displays an example of a fragment ion mass spectrum obtained from Substance P precursor ions, where the ion dissociation takes place within the above described flow reactor at essentially atmospheric pressure conditions. The spectrum contains a set of singly charged product ions with dominating b- and proposed to be c- fragments. The presence and intensity of the fragment ions depend on the temperature and gas flow through corona discharge. No fragmentation was observed for temperatures less than 350°C, after which the fragmentation efficiency increases roughly exponentially. We have observed that a reaction gas flow rate of 250–300 cm^3/min was optimal in terms of fragmentation efficiency. Since the total gas flow through the heated capillary of the LCQ “Classic” is 1020 cm^3/min, the optimal ratio of merging gas flows through the ESI and corona ion sources was ~ 3:1 for the present configuration of the flow reactor.

The occurrence of fragmentation was independent of the corona polarity. Fragmentation efficiency was directly proportional (up to certain threshold) to the current through the corona discharge. Notably, in terms of fragmentation efficiency the current-limiting regime was preferable with an optimal current through corona discharge of 100–200 μA. No fragment ions were observed without corona discharge.

The fragmentation occurred for a variety of gases (SO_2, Ar, N_2, O_2, etc) flowing through corona. No fragmentation was observed when helium was used as a reaction gas. The addition of water (H_2O) or hydrogen peroxide (H_2O_2) vapors to the corona discharge region significantly enhanced (up to ~100 times) the fragmentation efficiency, as it shown in Figure 3b. Although the majority of observed fragment ions were originated from the MH^+ precursor ions, also some sodium-cationized fragments were produced from the co-existing $[M+Na]^+$ ions. It is noteworthy to state that the ratio of c- to b- fragment ions was generally independent of H_2O/H_2O_2 vapor concentration in the corona discharge region, thus strongly indicating that c-ions are formed as opposed to oxidized forms of b-type ions.

In negative ESI mode, we have observed fragmentation patterns similar to the positive mode (series of c-, b- and y-fragments) but with more prominent y-and sometimes c- fragments. The representative fragment ion mass spectrum obtained from Substance P precursor ions in negative mode is shown in Figure 4.

The extensive fragmentation was also observed for a large variety of peptides and small proteins, including bradykinin, substance P, γ-endorphin, insulin, and melittin. Figure 5 shows an example of such fragment ion mass spectrum obtained in positive ESI mode from Bradykinin precursor ions.

In positive ESI mode, a charge reduction effect was observed with the negative corona discharge at flow reactor temperatures of less than 100°C (data not shown). Similar results were observed by the Lloyd Smith group [20] and were assigned to a charge neutralization reaction between ESI-generated peptide/protein cations and corona-generated anions. Noteworthy that a similar effect could be achieved just by heating the flow reactor without an ignition of corona discharge through the mechanism described earlier.

An addition of H_2O_2 vapors to the corona discharge region produced a sufficient intensity of fragment ions to attempt pseudo-MS^3 analysis, where the conventional CAD technique is applied in the 3-D ion trap to the accumulated precursor fragment ions (*e.g.* c-type) formed within the flow reactor. Figure 6 illustrates the quality of such pseudo-MS^3 mass spectrum acquired in a single scan. In this particular experiment, Substance P precursor ions were first dissociated within the flow reactor, and resulting fragment ions were accumulated (50 ms injection time) in the 3-D trap of LCQ “Classic”. Then the presumed c4+ fragment ion was isolated and subsequently fragmented using the conventional collision-activated dissociation technique. The resulting pseudo-MS^3 spectrum shows a series of b-, y- and a- ions as well as their ammonia or water losses, consistent with previous reports on CID of c-type ions [26, 27].

Suggested mechanism

The fact that the ion dissociation process is independent of the corona polarity implies a radical-induced mechanism of ion fragmentation. We suggest the following underlying scheme to describe the fragmentation, although a few other possibilities can be also hypothesized:

$$[M+H]^+ + OH^{\cdot} \rightarrow \text{fragments}$$
$$[M-H]^- + OH^{\cdot} \rightarrow \text{fragments} \quad (6)$$

In the suggested scheme the fragmentation is caused by hydroxyl radicals, which are common bi-products of the corona discharge. The likely source of OH radicals is water, via a reaction with a high-energy species produced in the corona discharge, such as the singlet-D oxygen atom:

$$O(^1D)+H_2O \rightarrow 2 \cdot OH^{\cdot} \quad (7)$$

In a typical experiment, electrospray is the source of water vapor. Adding water (H_2O) or hydrogen peroxide (H_2O_2) vapors directly to the gas flowing through the corona discharge dramatically increases the intensity of the fragments. This is one more sign in favor of a hydroxyl radical-induced dissociation (HRID).

The fact that hydroxyl radicals can cause backbone cleavage of peptides and proteins in the liquid and gas phases is well-known in biochemistry [28,29]. Cleavage of the protein results from hydroxyl-radical abstraction of the backbone C_α-H hydrogen atom. A C_α centered radical is generated that reacts with oxygen and leads to main-chain cleavage. At room temperature the rate of this initial abstraction (typically 10^7 $M^{-1}s^{-1}$) is much slower than the rate of reactions at side-chains (10^8–10^9 $M^{-1}s^{-1}$) [30,31]. The most frequent side-chain reaction is oxidation, preferentially observed at methionine and cysteine residues [32]. At room temperature, the main-chain cleavage reactions can be observed only if hydroxyl radicals are present at high doses [33–36]. We assume that an increase in temperature to 400°C (*i.e.*, significant vibrational activation) results in a significant increase in the rate of hydroxyl-radical abstraction that now significantly exceeds the rate of the side-chain reaction (although side-chain oxidation may be still present). Another interesting observation was the loss of 29 Da for Substance P ions (singly charged peptide and its fragments) and 30 Da for Bradykinin fragment ions, shown in Figures 3a and 5, respectively. MS/MS experiments on Bradykinin ion fragments confirmed that is related to the loss of CH_2O at the serine side chain. It is noteworthy to mention that ECD and ETD methods also have a propensity to lose small groups at different aminoacid residues (see Table 13.2 in [37]).

Since hydroxyl radicals are neutral species, their interaction with peptide and protein ions does not lead, unlike ECD and ETD processes, to direct charge reduction. As a result, the HRID pathway is feasible even for single-charged peptides. In our experiments, only singly charged precursor ions as well as all resulting fragment ions were observed in mass spectra at flow reactor temperatures higher than 380°C. However, with the existing design of the flow reactor, the possibility, that fragmentation takes place also for 2+ and 3+ peptide ions that may be present in small amounts within the flow reactor, can not be completely excluded.

Similar peptide fragmentation patterns were observed recently as a side-effect in Atmospheric Pressure Photoionization (APPI) source [38,39]. In APPI, peptide and proteins ions interact with a hot (400–450°C) reaction gas (“dopant”) undergoing irradiation by UV krypton lamp. Although the authors of these publications attempt to explain the mechanism of the observed phenomenon through either an electron transfer process or an interaction with free hydrogen radicals (contrary to work of Demirev [40]), we suggest the above described hydroxyl radical-induced mechanism where OH radicals are formed from water vapor by UV light. The aforementioned publications [38,39] also confirm c- and z- fragmentation patterns for single-charged peptide ions.

Conclusions and Future Directions

A novel method for peptide and protein fragmentation at atmospheric pressure is successfully demonstrated for a set of common peptides and small proteins. The fragmentation patterns

observed often contain c-type fragments that are specific to ECD/ETD, along with the y-/b-fragments that are specific to CAD. In the suggested mechanism, the fragmentation is caused by hydroxyl radicals that are common bi-products of corona discharge. The new dissociation method is equally efficient for positive as well as negative peptide and protein ions. Unlike ECD or ETD, the HRID technique seems to be directly applicable to single-charged ion species, since the fragmentation is induced by neutral radical species. A challenging aspect, however, is related to the fact that currently there is no capability for precursor ion selection. Also, the physical proximity of ion generation and ion/radical reaction regions holds some uncertainty in the charge state distribution of ions entering the flow reactor. These problems can be addressed if ion mobility [41,42] or field asymmetric waveform ion mobility [43,44] analyzers are interfaced between the atmospheric pressure ion source and the ion/radical flow reactor. This would allow users to selectively isolate target compounds based on a number of physical properties, including charge state and molecular conformation.

Acknowledgments

This work was supported by a SBIR grant from the National Institute of Health (1R43RR023224-01) to Science & Engineering Services Inc. (Columbia, MD). Authors thank Kevin Felber for his aid in engineering design and Dr. Thomas Saul for useful discussions.

References

1. Aebersold R, Goodlett DR. Mass spectrometry in proteomics. Chemical Reviews 2001;101:269. [PubMed: 11712248]
2. Bogdanov B, Smith RD. Proteomics by FTICR mass spectrometry: top down and bottom up. Mass Spectrometry Reviews 2005;24:168. [PubMed: 15389855]
3. Griffin TJ, Aebersold R. Advances in proteome analysis by mass spectrometry. J Biol Chem 2001;276:45497. [PubMed: 11585843]
4. Jennigs KR. The changing impact of the collision-induced decomposition of ions on mass spectrometry. International Journal of Mass Spectrometry 2000;200:479.
5. Kelleher NL. Top Down Proteomics. Analytical Chemistry 2004;76:197A. [PubMed: 14697051]
6. Resing KA, Ahn NG. Proteomics strategies for protein identification. FEBS Letters 2005;579:885. [PubMed: 15680968]
7. Wysocki VH, Resing KA, Zhang Q, Cheng G. Mass spectrometry of peptides and proteins. Methods 2005;35(3):211. [PubMed: 15722218]
8. Kaiser RE, Cooks RG, Syka JEP, Reynolds WE, Todd JFJ. Collisionally Activated Dissociation of Peptides Using a Quadrupole Ion Trap Mass Spectrometer. Rapid Communications in Mass Spectrometry 1990;4:30.
9. Haselmann KF, Budnik BA, Kjeldsen K, Polfer NC, Zubarev RA. Can the (M·-X) region in electron capture dissociation provide reliable information on amino acid composition of polypeptides? European Journal of Mass Spectrometry 2002;8:461.
10. Zubarev RA, Kelleher NL, McLafferty FW. Electron capture dissociation of multiply charged protein cations: A non-ergodic process. Journal of the American Chemical Society 1998;120:3265.
11. Chrisman PA, Pitteri SJ, Hogan JM, McLuckey SA. SO_2^- Electron Transfer Ion/Ion Reactions with Disulfide Linked Polypeptide Ions. Journal of the American Society for Mass Spectrometry 2005;16:1020. [PubMed: 15914021]
12. Pitteri SJ, Chrisman PA, McLuckey SA. Electron Transfer Ion/Ion Reactions of Doubly Protonated Peptides: The Effect of Elevated Bath Gas Temperature. Analytical Chemistry 2005;77:5662. [PubMed: 16131079]
13. Syka JEP, Coon JJ, Schroeder MJ, Shabanowitz J, Hunt DF. Peptide and protein sequence analysis by electron transfer dissociation mass spectrometry. Proceedings of the National Academy of Sciences 2004;101:9528.

14. Ogorzalek Loo RR, Udseth HR, Smith RD. A New Approach for the Study of Gas-Phase Ion-Ion Reactions Using Electrospray Ionization. Journal of American Society for Mass Spectrometry 1992;3:695.
15. Stephenson JL, McLuckey SA. Charge Manipulation for Improved Mass Determination of High Mass Species and Mixture Components by Electrospray Mass Spectrometry. Journal of Mass Spectrometry 1998;33:664. [PubMed: 9692249]
16. Ebeling DD, Westphall MS, Scalf M, Smith LM. Corona discharge in charge reduction electrospray mass spectrometry. Analytical Chemistry 2000;72:5158. [PubMed: 11080858]
17. Ebeling, DD.; Westphall, MS.; Scalf, M.; Smith, LM. New Method of Charge Reduction in Electrospray Mass Spectrometry. US patent 6,649,907.
18. Pui, DYH.; Chen, DR. Charged Particle Neutralizing Apparatus and Method of Neutralizing Charged Particles. US Patent 5,992,244.
19. Vilkov, AN.; Laiko, VV.; Misharin, AS.; Doroshenko, VM. ECD/ETD-type Fragmentation Induced at (or near) Atmospheric Pressure; Proceedings of the 55thASMS Conference on Mass Spectrometry and Allied Topics; Indianapolis, IN. 2007.
20. Frey BL, Lin Y, Westphall MS, Smith LM. Controlling gas-phase reactions for efficient charge reduction electrospray mass spectrometry of intact proteins. Journal of the American Society for Mass Spectrometry 2005;16:1876. [PubMed: 16198118]
21. Konenkov NV, Korolkov AN, Stepanov VA. Journal of Technical Physics 1996;66:176.(Russ)
22. Schneider BB, Baranov VI, Javaheri H, Covey TR. Particle discriminator. interface for nanoflow ESI-MS. Journal of the American Society for Mass Spectrometry 2003;14:1236. [PubMed: 14597113]
23. Rayleigh L. On the equilibrium of liquid conducting masses charged with electricity. Philosophical Magazine 1882;14:184.
24. Gomez A, Tang K. Charge and Fission of Droplets in Electrostatic Sprays. Physics of Fluids 1994;6:404.
25. Guggenheim, EA. Mixtures. Oxford University Press; London: 1952.
26. Han HL, Xia Y, McLuckey SA. Ion Trap Collisional Activation of c and z Ions Formed via Gas-Phase Ion/Ion Electron-Transfer Dissociation. Journal of Proteomic Research 2007;6:3062.
27. Mouls L, Subra G, Aubagnac JL, Martinez J, Enjalbal C. Tandem mass spectrometry of amidated peptides. Journal of Mass Spectrometry 2006;41:1470. [PubMed: 17072914]
28. Guan JQ, Chance MR. Structural proteomics of macromolecular assemblies using oxidative footprinting and mass spectrometry. Trends in Biochemical Sciences 2005;30(10):583. [PubMed: 16126388]
29. Maleknia SD, Wong JWH, Downard KM. Photochemical and Electrophysical Production of Radicals on Millisecond Timescales to Probe the Structure, Dynamics and Interactions of Proteins. Photochemical & Photobiological Sciences 2004;3:741. [PubMed: 15295629]
30. Hawkins CL, Davies MJ. Generation and propagation of radical reactions on proteins. Biochimica et Biophysica Acta 2001;1504:196. [PubMed: 11245785]
31. Buxton GV. Critical Review of Rate Constants for Reactions of Hydrated Electrons, Hydrogen Atoms and Hydroxyl Radicals in Aqueous Solution. Journal of Physical and Chemical Reference Data 1988;17:513.
32. Xu G, Kiselar J, He Q, Chance MR. Secondary reactions and strategies to improve quantitative protein footprinting. Analytical Chemistry 2005;77:3029. [PubMed: 15889890]
33. Maleknia SD, Ralston CY, Brenowitz MD, Downard KM, Chance MR. Determination of Macromolecular Folding and Structure by Synchrotron Radiolysis Techniques. Analytical Biochemistry 2001;289:103. [PubMed: 11161303]
34. Sharp JS, Becker JM, Hettich RL. Protein Surface Mapping by Chemical Oxidation: Structural Analysis by Mass Spectrometry. Analytical Biochemistry 2003;313:216. [PubMed: 12605858]
35. Heyduk E, Heyduk T. Mapping protein domains involved in macromolecular interactions: a novel protein footprinting approach. Biochemistry 2004;33:9643. [PubMed: 8068641]
36. Datwyler SA, Meares CF. Protein-protein interactions mapped by artificial proteases: where factors bind to RNA polymerase. Trends in Biochemical Sciences 2000;25:408–414. [PubMed: 10973050]

37. Zubarev, RA. Principles of mass spectrometry applied to biomolecules. Laskina, J.; Lifshitz, C., editors. Wiley; Hoboken, NJ: 2007.

38. Delobel A, Halgand F, Laffranchise-Gosse B, Sniijders H, Laprevote O. Characterization of hydrophobic peptides by atmospheric pressure photoionization-mass spectrometry and tandem mass spectrometry. Analytical Chemistry 2003;75:5961. [PubMed: 14588038]

39. Debois D, Giuliani A, Laprevote O. Fragmentation induced in atmospheric pressure photoionisation of peptides. Journal of Mass Spectrometry 2006;41:1554. [PubMed: 17094174]

40. Demirev PA. Generation of hydrogen radicals for reactivity studies in Fourier transform ion cyclotron resonance mass spectrometry. Rapid Communications in Mass Spectrometry 2000;14:777. [PubMed: 10825016]

41. Karasek FW. Plasma Chromatography. Analytical Chemistry 1974;46:710A. [PubMed: 4825961]

42. Eiceman, G.; Karpas, Z. Ion Mobility Spectrometry. CRC Press; Boca raton: 2005.

43. Purves RW, Guevremont R, Day S, Pipich CW, Matyjaszczyk MS. Mass spectrometric characterization of a high-field asymmetric waveform ion mobility spectrometer. Review of Scientific Instruments 1998;69:4094.

44. Buryakov IA, Krylov EV, Nazarov EG, Rasulev UK. A New Method Of Separation Of Multi-Atomic Ions By Mobility At Atmospheric Pressure Using A High-Frequency Amplitude-Asymmetric Strong Electric Field. International Journal of Mass Spectrometry and Ion Processes 1993;128:143.

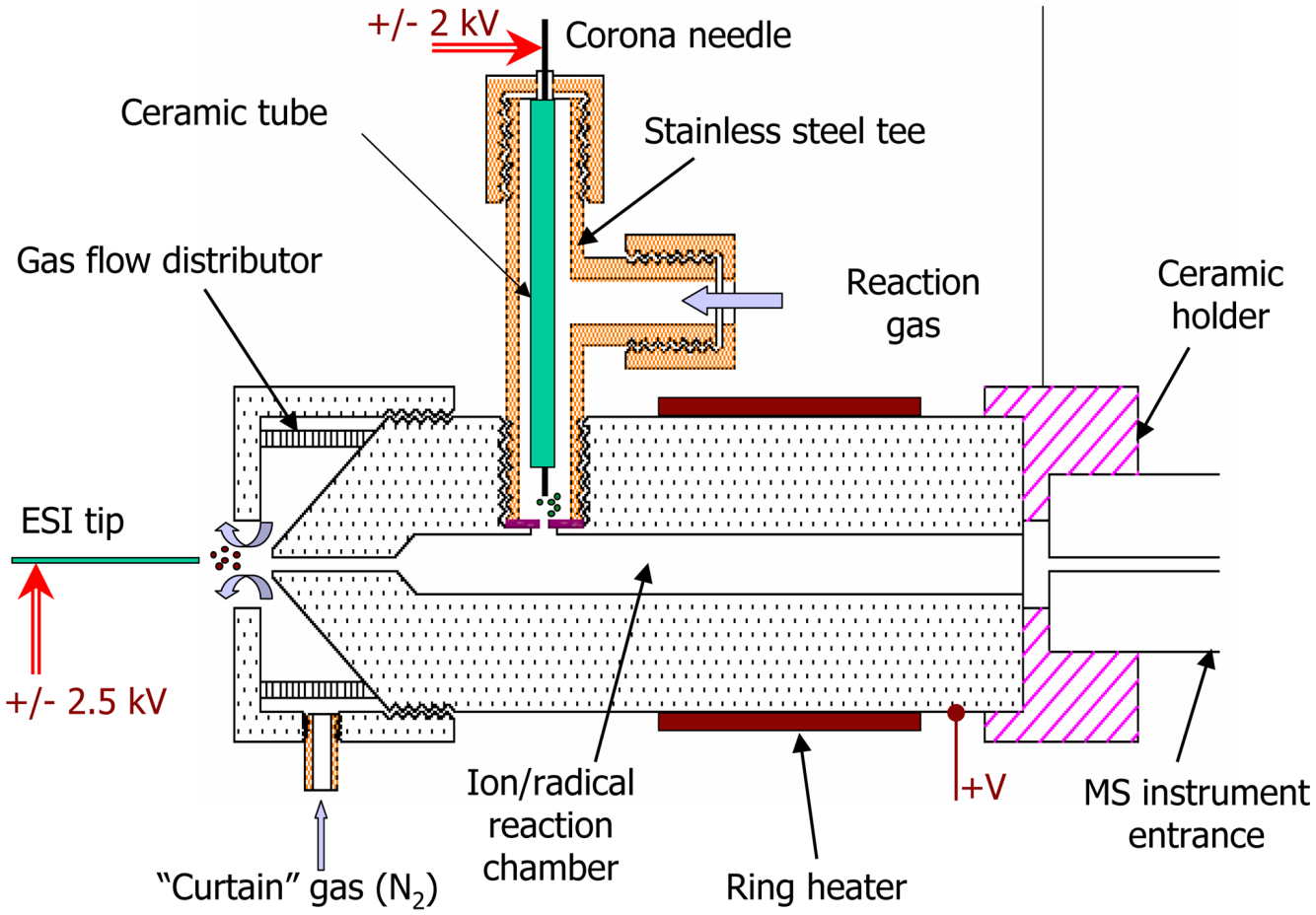

Figure 1.
Schematic diagram of the flow reactor installed onto the heated capillary of the MS instrument.

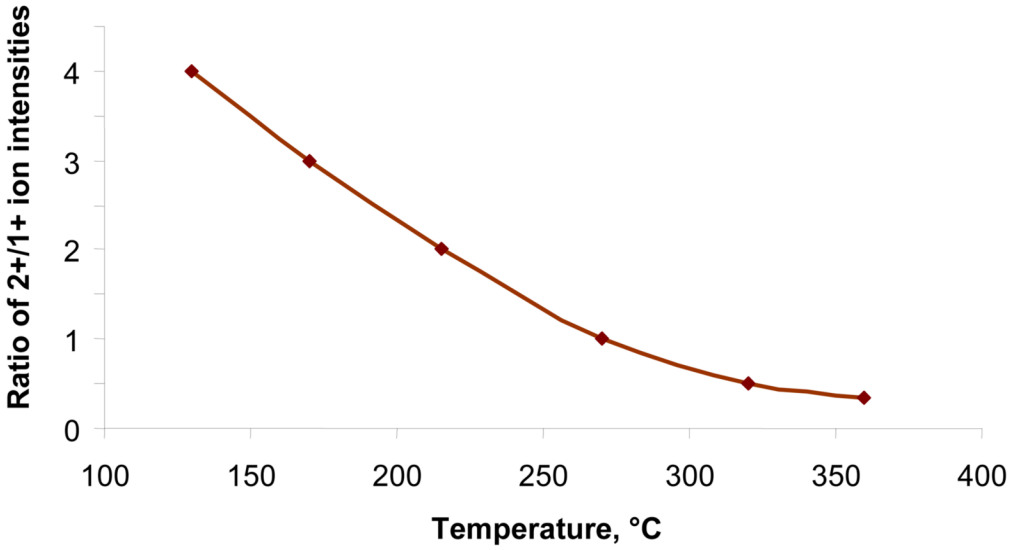

Figure 2.
The ratio dependence of the 2+/1+ charge state intensities of ESI-generated Substance P ions on flow reactor temperature.

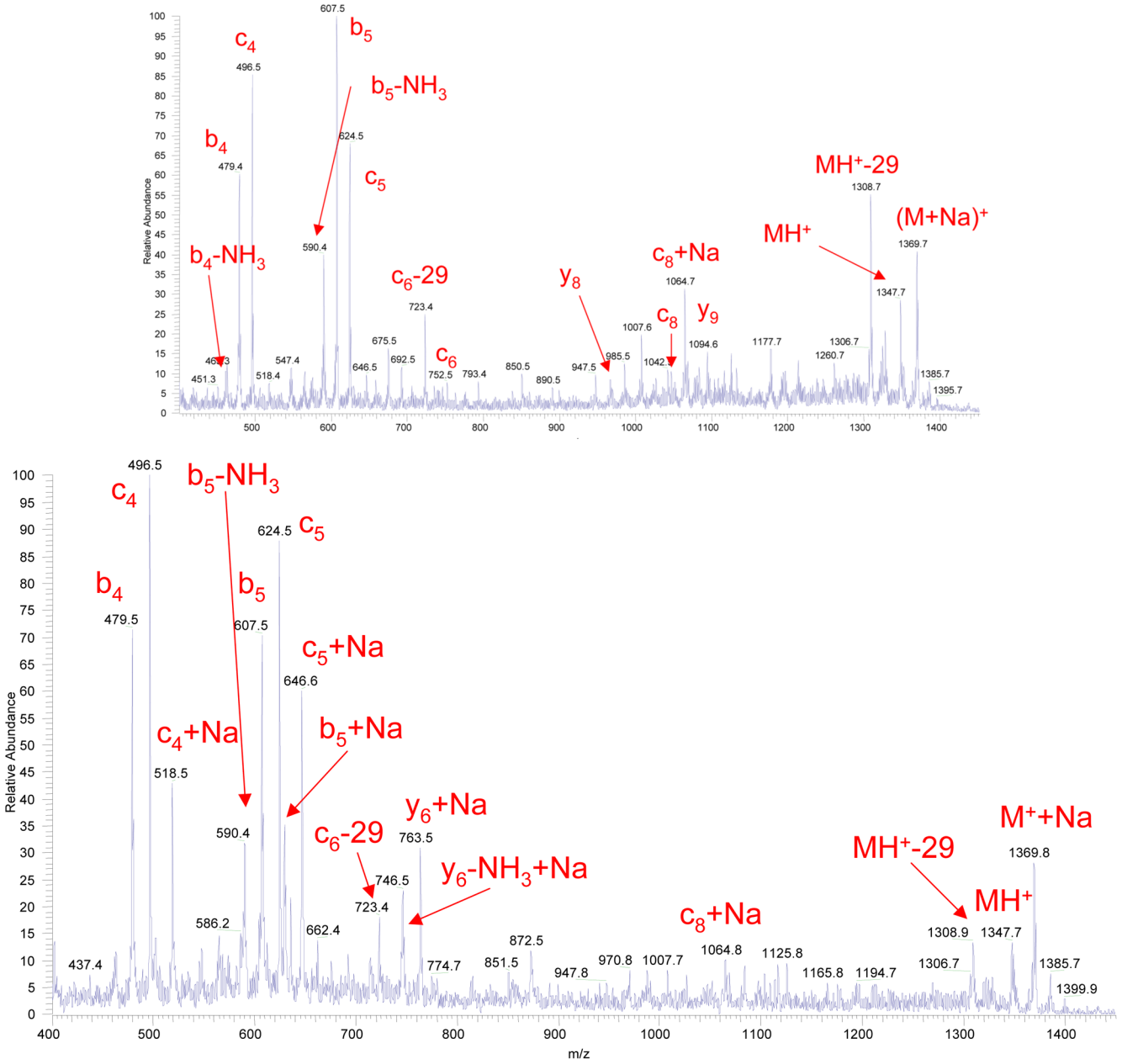

Figure 3.

Figure 3a. A fragment ion mass spectrum of Substance P, acquired by summing 50 scans. The corona discharge and electrospray had positive polarity. The flow reactor was maintained at a temperature of 420°C and the carrier gas (pure nitrogen) flow through the reactor was 280 cm^3/min.

Figure 3b. A fragment ion mass spectrum of Substance P, acquired in a single scan. The corona discharge and electrospray had positive polarity. The flow reactor was maintained at a temperature of 420°C and the carrier gas (pure nitrogen with an addition of H_2O_2 vapor) flow through the reactor was 280 cm^3/min.

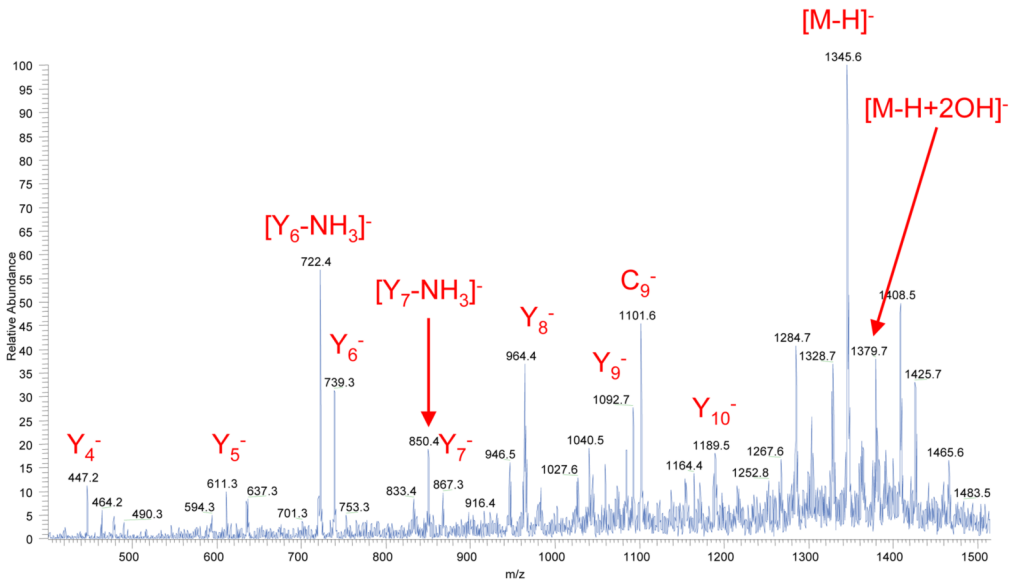

Figure 4.

A fragment ion mass spectrum of Substance P, acquired in a single scan. The corona discharge had positive polarity and electrospray had negative polarity. The flow reactor was maintained at a temperature of 420°C and the carrier gas (pure nitrogen with an addition of H_2O_2 vapor) flow through the reactor was 280 cm^3/min.

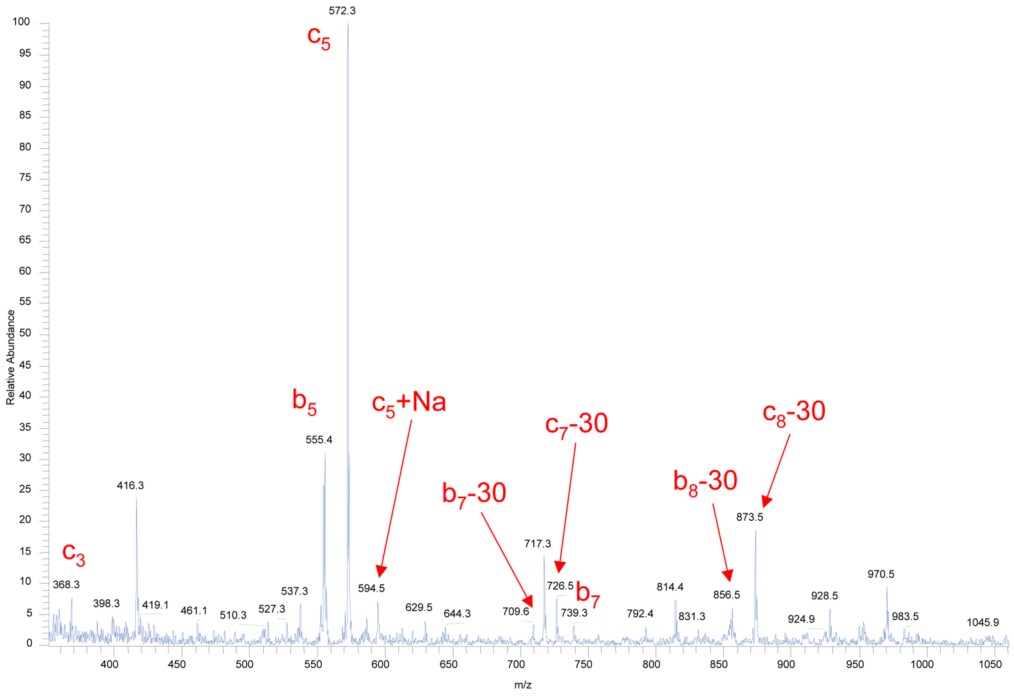

Figure 5.

A fragment ion mass spectrum of Bradykinin, acquired in a single scan. The corona discharge and electrospray had positive polarity. The flow reactor was maintained at a temperature of 400°C and the carrier gas (pure nitrogen with an addition of H_2O_2 vapor) flow through the reactor was 250 cm^3/min.

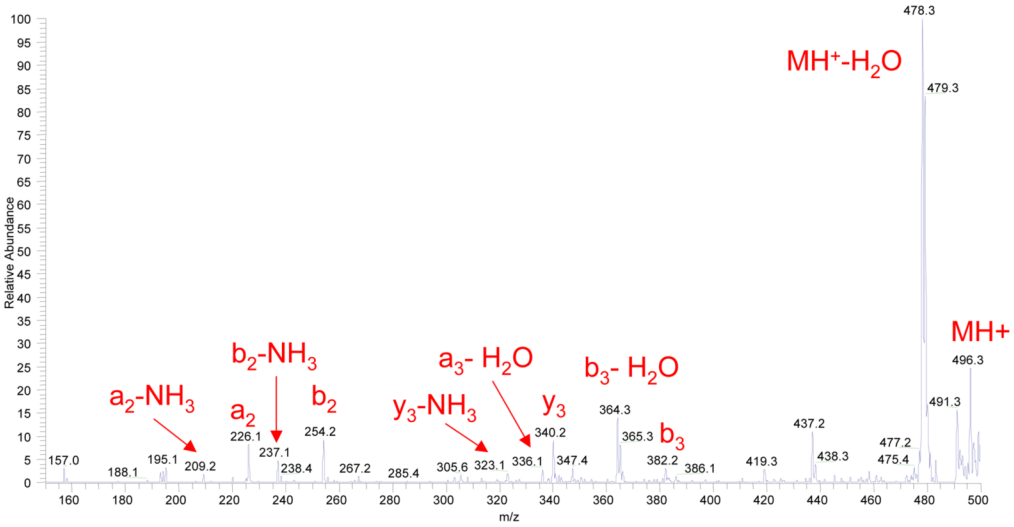

Figure 6.

Pseudo-MS^3 mass spectrum obtained from Substance P precursor ions by combination of the fragmentation within the flow reactor and the conventional CAD MS/MS on c4+ fragment (*m/z* = 496.1) generated in the first fragmentation step.